

## Parametric Driving of Dark Solitons in Atomic Bose-Einstein Condensates

N. P. Proukakis<sup>y</sup>, N. G. Parker<sup>y</sup>, C. F. Barenghi<sup>z</sup>, and C. S. Adams<sup>y</sup><sup>y</sup> Department of Physics, University of Durham,  
South Road, Durham, DH1 3LE, United Kingdom and<sup>z</sup> School of Mathematics and Statistics, University of Newcastle,  
Newcastle upon Tyne, NE1 7RU, United Kingdom

A dark soliton oscillating in an elongated harmonically-confined atomic Bose-Einstein condensate continuously exchanges energy with the sound field. Periodic optical ‘paddles’ are employed to controllably enhance the sound density and transfer energy to the soliton, analogous to parametric driving. In the absence of damping, the amplitude of the soliton oscillations can be dramatically reduced, whereas with damping, a driven soliton equilibrates as a stable soliton with lower energy, thereby extending the soliton lifetime up to the lifetime of the condensate.

PACS numbers: 03.75.Lm, 05.45.Yv, 42.81.Dp and 47.35.+i

Dark solitons [1] are an important manifestation of the intrinsic nonlinearity of a system and arise in diverse systems such as optical fibers [2], waveguides [3], surfaces of shallow liquids [4], magnetic films [5], and atomic Bose-Einstein Condensates (BECs) [6]. Dark solitons are known to be dynamically unstable in higher than one-dimensional (1D) manifolds (e.g. snake instability in 3D systems leading to a decay into vortex rings [7, 8]). Solitons in 1D geometries experience other instabilities, whose nature depends on the details of the system: For example, dark solitons in optical media are prone to nonlinearity-induced changes in the refractive index [1], whereas in harmonically trapped atomic BECs they experience dynamical instabilities due to the longitudinal component [9, 10, 11, 12, 13, 14, 15], as well as thermodynamic [16] and quantum [17] effects. Instabilities lead to dissipation, which manifests itself in the emission of radiation. Compensation against dissipative losses by parametric driving has been demonstrated in some of the above media [4, 18]. The aim of this Letter is to discuss this effect in the context of atomic BECs.

In atomic gases, the snake instability [8] can be suppressed in elongated, quasi-one-dimensional (quasi-1D) geometries [19], and thermal instabilities are minimized at very low temperatures  $T \ll T_c$  (where  $T_c$  is the BEC transition temperature). In this limit, a dark soliton oscillating in a harmonically confined BEC continuously emits its radiation (in the form of sound waves) due to the inhomogeneous background density [9]. The sound remains confined and re-interacts with the soliton, leading to periodic oscillations of the soliton energy [13]. In this Letter we propose the controlled amplification of the background sound field, and illustrate the resulting transfer of energy into the soliton, in close analogy to established parametric driving techniques [4]. Energy is pumped into the sound field via periodically-modulated ‘paddles’, located towards the condensate edge (Fig. 1). If the drive frequency is nearly resonant with the soliton oscillation frequency, one observes significant energy transfer to the soliton. In the absence of dissipation, this leads to a dramatic reduction in the amplitude of the soliton oscillations. Under dissipative conditions, the

damped soliton equilibrates as a stable soliton with lower energy, with its lifetime extended up to the condensate lifetime. Moreover, suitable engineering of the phase of the driving field (relative to the soliton oscillations) can maintain the soliton energy at its initial value for times significantly longer than the undriven soliton lifetime.

Our analysis is based on the cylindrically-symmetric 3D Gross-Pitaevskii Equation (GPE) describing the evolution of the macroscopic order parameter  $\psi(z)$  of an elongated 3D atomic BEC

$$i\hbar \frac{\partial \psi}{\partial t} = -\frac{\hbar^2}{2m} \nabla^2 \psi + V \psi + g |\psi|^2 \psi \quad (1)$$

where  $m$  is the atomic mass,  $V = V_T(x) + V_D(x)$ ,  $V_T(x) = (m/2)(\omega_z^2 z^2 + \omega_\perp^2 r^2)$  is the harmonic confining potential of longitudinal (transverse) frequency  $\omega_z$  ( $\omega_\perp$ ), where  $\omega_z = \hbar^{-1} \epsilon_z$ , and  $V_D(x)$  is the drive potential (Eq. (3)). The nonlinearity arises from atomic interactions yielding a scattering amplitude  $g = 4\pi\hbar^2 a/m$ , where  $a$  is the s-wave scattering length. In this work,  $a > 0$ , i.e. effective repulsive atomic interactions. The chemical potential is given by  $\mu = gn_0$ , where  $n_0$  is the peak atomic density.

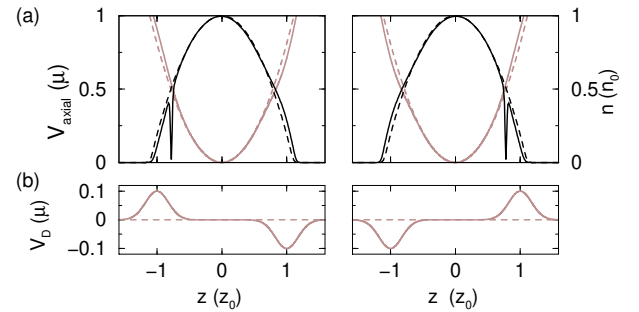


FIG. 1: Schematic of parametric driving: (a) Total axial potential (grey lines, left axis) and density (black lines, right axis) of perturbed harmonic trap with propagating dark soliton (solid lines), at two times (left/right plots) corresponding to maximum drive amplitudes. (b) Corresponding drive potentials (black,  $> 0$ ). Dashed grey lines denote density of unperturbed harmonic trap, while dashed black lines indicate corresponding density.

Dark soliton solutions are supported by the 1D form of Eq. (1) in the absence of external confinement ( $V = 0$ ). On a uniform background density  $n$ , a dark soliton with speed  $v$  and position  $(z - vt)$  has the form,

$$\psi(z; t) = \sqrt{\frac{P}{n}} e^{i(\phi - \omega t)} \tanh \left( \frac{z - vt}{\xi} \right) + i \frac{v}{c} \quad (2)$$

where  $\xi = \frac{1}{\sqrt{2} \sqrt{1 - (v/c)^2}}$ , and the healing length  $\xi = \sqrt{\frac{\hbar^2}{2m\mu}}$  characterises the soliton width. The soliton speed  $v = c \sqrt{1 - (n_d/n)^2} = \cos(S/2)$  depends on the total phase slip  $S$  across the centre and the soliton depth  $n_d$  (with respect to the background density), with the limiting value set by the Bogoliubov speed of sound  $c = \sqrt{\mu/m}$ . The energy of the unperturbed dark soliton of Eq. (2) is given by  $E_s^0 = (4/3) \sim c n (1 - (v/c)^2)^{3/2}$ . The drive potential

$$V_D = \frac{\hbar}{2} \sin(\Omega_D t) e^{-(z+z_0)^2/w_0^2} - \frac{\hbar}{2} e^{-(z-z_0)^2/w_0^2} \quad (3)$$

consists of two periodically modulated gaussian ‘paddles’, with amplitude  $\frac{\hbar}{2}$ , at positions  $\pm z_0$ , oscillating in anti-phase at a fixed frequency  $\Omega_D$ , close to the soliton frequency (Fig. 1). Such a set-up could be created by time-dependent red and blue detuned laser beams with beam waist  $w_0$ .

In our work, the dark soliton is defined as the density deviation from the unperturbed density (in the absence of the soliton) within the ‘soliton region’  $R: [z_s - 5; z_s + 5]$ , where  $z_s$  the instantaneous position of the local density minimum. Such a ‘perturbed’ soliton includes sound excitations located within the soliton region at any time. The motion and stability of a quasi-1D dark soliton is well parametrized by its energy. In order to facilitate a direct comparison of the quasi-1D soliton decay to the analytical homogeneous 1D soliton energy, the soliton dynamics are parametrized in terms of the ‘on-axis’ ( $\phi = 0$ ) soliton energy  $E_s = \int_R f''[|\psi|^2] - f''[b_g(0; z)] dz$ , where  $f''(|\psi|^2) = \frac{1}{2} (2m)^{-1} \dot{\psi}^2 + V \psi^2 + (g/2) \psi^4$  and  $f''[b_g(0; z)]$  is the corresponding energy contribution of the background fluid [13, 14, 20].

**Dissipationless Regime:** Consider first the case of no dissipation (Eq. (1)). In the absence of  $V_D$ , the soliton oscillates at  $\omega_{s0} = \omega_z = \frac{1}{2} [9, 10, 11, 12, 13, 14, 15, 16]$ , emitting sound waves which oscillate at the trap frequency  $\omega_z$ . This frequency mismatch means that the soliton propagates through a periodically modulated background density, leading to a weak periodic modulation of the soliton energy (Fig. 2(a), curves (i)). The amplitude of this modulation is enhanced by the coupling between longitudinal and transverse degrees of freedom [11, 13].

To demonstrate substantial energy transfer into the soliton, we start with a low energy shallow soliton (speed  $v_0 = 0.75c$  at  $z = 0$ ). Applying the drive potential induces an additional periodic background density modulation and a time-dependence in the soliton oscillation

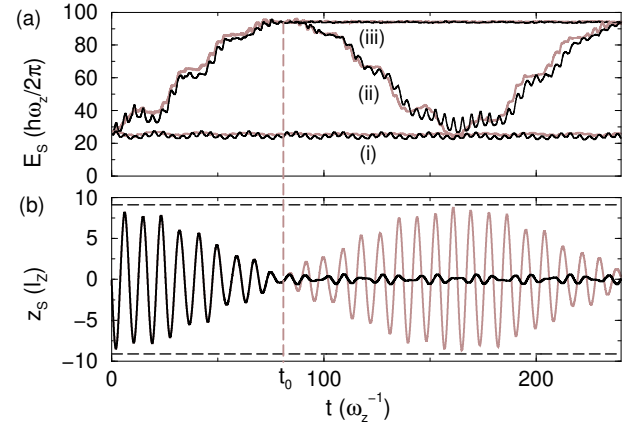


FIG. 2: On-axis quasi-1D soliton energy for (i) undriven case, (ii) continuous driving and (iii) driving switched on at  $t_0 = 80 \omega_z^{-1}$ , based on simulations of the 3D cylindrically-symmetric GPE (black lines) and 1D GPE (grey lines) for a soliton with initial speed  $v = 0.75c$ . (b) Longitudinal soliton oscillations with continuous driving (grey line), and driving switched on at  $t_0$  (vertical grey line) under the 3D GPE. Dashed lines indicate corresponding amplitude in absence of driving. The trap strength is determined from the chemical potential of the system: Quasi-1D:  $\mu_{3D} = 8\mu$  where  $\mu = (\frac{1}{2} \dot{\psi}^2)^{1/3}$  and  $\mu_z = \mu_z = 250$ . Pure 1D:  $\mu_{1D} = 70\mu_z$  for which the 1D density matches the quasi-1D longitudinal density. Drive parameters:  $\Omega_D = 0.98\omega_{s0}$ ,  $w_0 = 32l_z$  and  $z_0 = 10.7l_z$  where  $l_z = \frac{1}{\sqrt{2} \sqrt{1 - (v/c)^2}}$  the longitudinal harmonic oscillator length.

frequency, which is found to vary by no more than 10% around its unperturbed value  $\omega_{s0}$ . As a result, the relative phase between the drive and the soliton oscillations, which determines the direction of energy flow between soliton and sound, becomes time-dependent. Beginning with the drive out-of-phase with the soliton oscillations, the soliton initially acquires energy, up to time  $t_0$ , after which it begins to lose energy, and the cycle repeats, as shown by curves (ii) in Fig. 2(a). This figure illustrates the good agreement between the 3D ‘on-axis’ energy (black lines) and the corresponding energy of the pure 1D simulations (grey lines) (the 3D results feature an additional small amplitude oscillation due to longitudinal-transverse coupling). The corresponding beating in the soliton oscillation amplitude is shown in Fig. 2(b) (grey line). This beating effect can be visualized as the periodic cycling between the initial low energy dark soliton, and the nearly stationary high energy soliton. This picture is analogous to the cycling of a driven condensate between the ‘ho-vortex’ and ‘single-vortex’ configurations [22].

A soliton of higher energy can be created by removing the drive potential after a certain pumping time. In general, stopping the drive at an arbitrary point in the energy gain-loss cycle, will lead to stabilization around that energy, with associated residual oscillations. In order to create a nearly stationary soliton (black line in Fig. 2(b)), one must stop the drive when the soliton

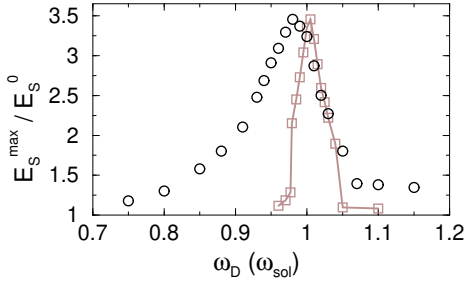


FIG. 3: Ratio of maximum pumped energy  $E_s^{\max}$  to initial soliton energy  $E_s^0$  for a soliton with initial speed  $v_0 = 0.75c$  in the presence of optimized driving as a function of drive frequency  $\omega_D$  (in units of the unperturbed soliton frequency  $\omega_{\text{sol}} = \omega_z/2$ ) for (i) no damping (black circles), or (ii) with damping  $\gamma = 5 \cdot 10^{-4}$  (grey squares). This value of  $\gamma$  leads to the same soliton lifetime as for the undriven  $0.3c$  soliton in Fig. 4. Results based on pure 1D GPE for the case of Fig. 2.

has acquired its maximum energy, for which the energy oscillations are suppressed (curve (iii) in Fig. 2(a)).

The soliton dynamics depend rather sensitively on the parameters of the driving field which should be carefully optimized for these effects to be clearly observable. Firstly, the pumping should take place outside of the range of the soliton oscillations (i.e.  $z_0 > 9l_z$  for  $v_0 = 0.75c$ ). If this is not the case, the soliton traverses the gaussian bumps, leading to ‘dephasing’ of emitted sound waves and subsequent decay of the soliton [14]. The transfer of energy between the soliton and the sound field depends on the phase of the drive relative to the soliton oscillations, and hence on the drive potential seen by the soliton at the extrema of its oscillatory motion. This parameter depends in turn not only on the drive frequency  $\omega_D$ , but also on the amplitude of the potential modulation  $\epsilon$ , the range of the potential  $w_0$ , its location  $z_0$ , and the initial soliton speed  $v_0$ . If all but one of the above parameters are kept constant, then there is a resonance around an optimum value of that parameter. This resonance is illustrated for the drive frequency  $\omega_D$  by the open circles in Fig. 3. Note that the maximum pumping does not arise at  $\omega_{\text{sol}}$ , due to the additional frequency modulation induced by the perturbing potential; however, the optimum frequency is consistently found to lie close to the unperturbed frequency. Importantly, the width of the resonance for which the transferred soliton energy reaches half its maximum value (FWHM), is reasonably broad, of the order of 10% the soliton frequency. We have also investigated alternative schemes for pumping energy into the system. For example, using one off-centre paddle, or inverting the sign in Eq. (3) (i.e.  $\epsilon < 0$ ), leads to a delayed and less efficient energy transfer, while periodically displacing the trap leads to no net increase in the soliton energy.

**Dissipative Regime:** In a realistic quasi-1D system featuring suppressed snake-instability [8], both the condensate and the soliton will be prone to damping, e.g.

due to the presence of a small thermal cloud [16]. A first estimate into the effect of dissipation can be obtained by introducing a phenomenological damping term  $\sim \partial_t \psi$  on the left hand side of Eq. (1). In the absence of driving, this term leads to an approximately exponential decay of the soliton energy, modified by the oscillatory motion of the soliton (dashed lines in Fig. 4(a)). Dissipation also damps both the sound field, leading to a narrowing of the resonance in the drive frequency, and a shift of the resonant frequency towards the unperturbed soliton frequency (grey data in Fig. 3).

**Stabilization Against Decay:** For a high energy soliton, continuous parametric driving counterbalances damping initially (solid line in Fig. 4(a) up to  $\omega_z t \approx 90$ ), but subsequently the soliton starts to decay ( $90 < \omega_z t < 170$ ), thereby changing both the amplitude and the phase of the soliton oscillations [9, 13]. The evolution in the relative phase between the drive and the soliton oscillations eventually enables the soliton to gain energy again. After a few such gain-loss cycles, the initial deep  $v_0 = 0.3c$  soliton finally equilibrates as a shallower soliton of energy  $E \approx 35\omega_z$  (corresponding to  $v_0 \approx 0.7c$ ).

**Stabilization at Fixed Energy:** Some applications may require a soliton to be maintained at a fixed energy. For this, one must balance the competing effects of driving

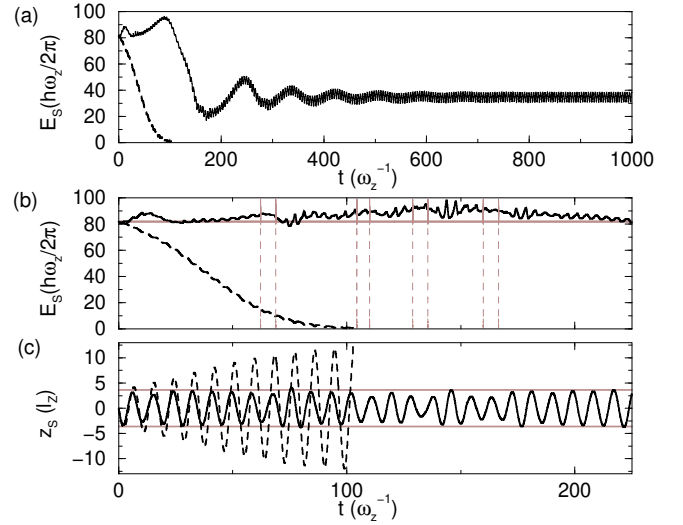


FIG. 4: (a) Soliton energy (initial speed  $v_0 = 0.3c$ ) for a dissipative system ( $\gamma = 10^{-3}$ ) in the presence (solid line) or absence (dashed) of continuous driving ( $\omega_D = \omega_{\text{sol}}$ ,  $z_0 = 7.1l_z$ ). The driven soliton stabilizes at  $E \approx 35\omega_z$ , corresponding to  $v_0 \approx 0.7c$ . (b) Energy of a  $v_0 = 0.3c$  soliton with parametric driving (solid black), with a sequence of rephasing cycles during the periods between adjacent dashed grey lines. Corresponding curves in the absence of driving are also shown for a dissipative ( $\gamma = 10^{-3}$ , dashed black) and a non-dissipative  $v_0 = 0.3c$  soliton (solid grey). (c) Driven (solid) and undriven (dashed) soliton trajectories in the presence of dissipation for case (b). Horizontal grey lines indicate the corresponding undamped undriven amplitude of soliton oscillations. Results based on the 1D GPE, with other parameters as in Fig. 2.

and dissipation. This can be achieved by rephasing the drive relative to the soliton oscillations at appropriate times, as demonstrated by the solid line in Fig. 4(b) for a sequence of four rephasing operations. In principle, this rephasing can be extended to the duration of the condensate lifetime. In an experiment, one actually measures the position of the soliton (rather than its energy) [6]. Hence, rephasing could be performed by monitoring the amplitude of the soliton oscillations and adjusting the drive phase, so that the soliton oscillation amplitude remains constant. Fig. 4(c) shows the oscillation amplitude of the parametrically driven soliton (solid black line), which is very similar to the undamped undriven case (horizontal grey lines), and is clearly distinct from the undriven dissipative motion (dashed lines), whose amplitude increases until the soliton decays at  $z/t = 105$ .

Finally, we discuss the relevance of the proposed scheme to current experiments with atomic BECs. Given a longitudinal confinement  $\omega_z = 2 \times 10$  Hz, the presented results correspond to  $\omega_p = 2 \times 2500$  Hz and a linear on-axis density  $n = 5 \times 10^7 (1.5 \times 10^7) \text{ m}^{-1}$  of  $^{23}\text{Na}$  ( $^{87}\text{Rb}$ ). The harmonic oscillator time unit is 15 ms. In the dissipative example of Fig. 4 with  $\gamma = 10^{-3}$ , this would correspond to a soliton lifetime of around 1 s, which is consistent with the theoretical predictions for solitons in highly elongated three-dimensional ge-

ometries [9, 10, 16]. The paddle beams have a waist  $w_0 = 20 \text{ }\mu\text{m}$  and maximum amplitude  $\omega = 7 \times \omega_z$  located around  $z_0 = 7l_z$ . We have also verified that the results presented here hold for smaller aspect ratios (e.g.  $\omega_p/\omega_z = 50$ ). Since, for a given aspect ratio, higher frequencies correspond to faster timescales, the technique presented here is not sensitive to the particular soliton lifetime. Increasing, however, beyond an upper limit (corresponding to large dissipation), renders it practically impossible to pump energy into the system.

In summary, we have shown that, in the case of a dark soliton oscillating in a harmonically trapped Bose-Einstein condensate, the addition of two out-of-phase gaussian potentials, with amplitude modulated periodically at a fixed frequency close to the soliton frequency, pumps energy into the soliton. This technique, which bears close analogies to parametric driving, can stabilize the soliton against decay for timescales comparable to the condensate lifetime. Furthermore, suitable optimization of the phase of the drive can force the soliton to maintain its initial energy for at least a few times its natural lifetime. Both effects should be experimentally observable in current experiments.

We acknowledge discussions with D.J. Frantzeskakis and P.G. Kevrekidis and the UK EPSRC for funding.

- 
- [1] Y. S. Kivshar and B. Luther-Davies, *Phys. Rep.* 278, 81-197 (1998).
  - [2] D. K. Rokel, N. J. Halas, G. Giuliani, and D. G. Risckowsky, *Phys. Rev. Lett.* 60, 29 (1998).
  - [3] G. A. Swartzlander Jr. et al., *Phys. Rev. Lett.* 66, 1583 (1991).
  - [4] B. Denardo, W. W. Right, S. Puttermann, and A. Larraz, *Phys. Rev. Lett.* 64, 1518 (1990).
  - [5] M. Chen, M. A. T. Sankov, J. M. Nash, and C. E. Patton, *Phys. Rev. Lett.* 70, 1707 (1993).
  - [6] S. Burger et al., *Phys. Rev. Lett.* 83, 5198 (1999); J. Denschlag et al., *Science* 287, 97 (2000); Z. Dutton, M. Budde, C. Slowe, and L. V. Hau, *Science* 293, 663 (2001).
  - [7] A. V. Mamaev, M. S. Manan, and A. A. Zozulya, *Phys. Rev. Lett.* 76, 2262 (1996).
  - [8] D. L. Feder et al., *Phys. Rev. A* 62, 053606 (2000); B. P. Anderson et al., *Phys. Rev. Lett.* 86, 2926 (2001); J. Brand and W. Reinhardt, *Phys. Rev. A* 65, 043612 (2002).
  - [9] T. Busch and J. R. Anglin, *Phys. Rev. Lett.* 84, 2298 (1999).
  - [10] A. E. M. Muryshv, H. B. van Linden van den Heuvell, and G. V. Shlyapnikov, *Phys. Rev. A* 60, R2665 (1999).
  - [11] G. Huang, J. Szeftel, and S. Zhu, *Phys. Rev. A* 65, 053605 (2002).
  - [12] D. J. Frantzeskakis et al., *Phys. Rev. A* 66, 053608 (2002).
  - [13] N. G. Parker, N. P. Proukakis, M. Leadbeater, and C. S. Adams, *Phys. Rev. Lett.* 90, 220401 (2003).
  - [14] N. G. Parker, N. P. Proukakis, M. Leadbeater, and C. S. Adams, *J. Phys. B* 36, 2891 (2003); N. G. Parker et al., *J. Phys. B* 37, S175 (2004); N. P. Proukakis et al., *J. Opt. B* 6, S380 (2004).
  - [15] V. A. Brazhnyi and V. V. Konotop, *Phys. Rev. A* 68, 043613 (2003).
  - [16] P. O. Fedichev, A. E. Muryshv and G. V. Shlyapnikov, *Phys. Rev. A* 60, 3220 (1999); A. E. Muryshv et al., *Phys. Rev. Lett.* 89, 110401 (2002).
  - [17] J. D. Ziamaga et al., *J. Phys. B* 36, 1217 (2003).
  - [18] C. E. Liphick and E. Meron, *Phys. Rev. A* 40, 3226 (1989); F. K. Abdullaev and S. K. Tadjimuratov, *Opt. Comm.* 116, 179 (1995); A. D. Kim, W. L. Kath and C. G. Goedde, *Opt. Lett.* 21, 465 (1996); P. Couillet et al., *Phys. Rev. Lett.* 65, 1352 (1990); D. V. Skryabin et al., *Phys. Rev. E* 64, 056618 (2001); I. V. Barashenkov, S. R. Woodford and E. V. Zemlyanaya, *Phys. Rev. Lett.* 90, 054103 (2003).
  - [19] A. G. Oerlitz et al., *Phys. Rev. Lett.* 87, 130402 (2001); F. Schreck et al., *Phys. Rev. Lett.* 87, 080403 (2001); H. Ott et al., *Phys. Rev. Lett.* 87, 230401 (2001).
  - [20] L. D. Carr, J. Brand, S. Burger, and A. Sanpera, *Phys. Rev. A* 63, 051601 (2001).
  - [21] S. Choi, S. A. Morgan and K. Burnett, *Phys. Rev. A* 57, 4057 (1998); M. Tsubota, K. Kasamatsu and M. Ueda, *Phys. Rev. A* 65, 023603 (2002).
  - [22] B. M. Caradoc-Davies, R. J. Ballagh and K. Burnett, *Phys. Rev. Lett.* 83, 895 (1999).